AG
EDITOR

**ORIGINAL**

# Improving cooling rate in a cold room by using a parametric study coupled with computational fluid dynamics

## Mejora de la velocidad de enfriamiento en una cámara frigorífica mediante un estudio paramétrico acoplado con dinámica de fluidos computacional

Wilmer Cruz Guayacundo[1] ✉, Natali López Mejía[2] ✉, Hugo Fabian Lobatón García[3] ✉, Dustin Tahisin Gómez Rodríguez[4] ✉

[1]Faculty of Engineering, Universitaria Agustiniana. Bogotá 110811, Colombia.

[2]Division of Food Technology, Universitaria Agustiniana. Bogotá 110811, Colombia.

[3]Research Directorate. Bogotá 110811, Colombia.

[4]Research Directorate.

**ABSTRACT**

The cooling dynamics of fruits depend on the flow conditions around the biological material. Computational fluid dynamics (CFD) coupled with a design of experiments (DOE) was implemented to reveal how a design variable (bin open area) and an operational variable (cold air mass flow at the inlet) affect turbulence and therefore the cooling kinetics. The CFD model was first validated against experimental local velocities inside the bins with an error of 14 % to later be used in the parametric study (simulated data was consistent with experimental data). A clear non-homogeneity in turbulence distribution (vertical stratification) was found and therefore different local cooling rates. For this cooling room, the bin located in the top are cooling faster (8,1 hour 7/8th cooling time) that the bin located in the bottom (14,7 hours 7/8th cooling time). A 65 % reduction in the mass flow rate shows a 21 % increment in 7/8th cooling time and 57 % increment in the lateral bin open area with a constant the flow rate, shows 9 % increments in the 7/8th cooling time but with a 2 hours (7/8th cooling time) reduction in the difference between the bin in the top and the bin in the bottom which implied better homogeneity.

**Keywords:** Precooling; CFD; Effective Thermal Conductivity; Cooling Kinetics.

**RESUMEN**

La dinámica de enfriamiento de las frutas depende de las condiciones de flujo alrededor del material biológico. Se implementó dinámica de fluidos computacional (CFD) junto con un diseño de experimentos (DOE) para revelar cómo una variable de diseño (área abierta del contenedor) y una variable operativa (flujo másico de aire frío en la entrada) afectan la turbulencia y, por lo tanto, la cinética de enfriamiento. El modelo de CFD se validó inicialmente frente a velocidades locales experimentales dentro de los contenedores con un error del 14 % para posteriormente utilizarse en el estudio paramétrico (los datos simulados fueron consistentes con los datos experimentales). Se observó una clara falta de homogeneidad en la distribución de la turbulencia (estratificación vertical) y, por lo tanto, diferentes velocidades de enfriamiento local. En esta cámara de enfriamiento, el contenedor ubicado en la parte superior se enfría más rápido (8,1 horas y 7/8 de tiempo de enfriamiento) que el contenedor ubicado en la parte inferior (14,7 horas y 7/8 de tiempo de enfriamiento). Una reducción del 65 % en el caudal másico muestra un incremento del 21 % en el tiempo de enfriamiento de 7/8 y del 57 % en el área abierta lateral del contenedor con un caudal constante.

Esto muestra incrementos del 9 % en el tiempo de enfriamiento de 7/8, pero con una reducción de 2 horas (tiempo de enfriamiento de 7/8) en la diferencia entre el contenedor superior y el contenedor inferior, lo que implica una mejor homogeneidad.

**Palabras clave:** Preenfriamiento; CFD; Conductividad Térmica Efectiva; Cinética de Enfriamiento.

## INTRODUCTION

Food is a complex matrix composed of a set of substances that, independently, have physicochemical properties contributing to the overall properties of food. So that food reaches the consumer's table, it goes through a series of links, the first link is the primary production (agricultural production), which includes all the subsequent harvest treatment, which is decisive either because it will be exported, because it will be transformed into a value-added product or because it will be used for the fresh consumption. To reach the second links in the food chain with the best conditions, the treatment after the harvest must be carried out in such a way that the respiratory process is delayed, this delay leads to a series of physicochemical, microbiological, and enzymatic reactions[1] and it is achieved through pre-cooling with which the heat that the fruit brings from the field is reduced.[2]

As a result of the precooling, the high percentages of food loss are reduced in fruits and vegetables, that decrease in the loss goes from 13 to 38 %.[3] This is the beginning of the cold chain to which the perishable foods are subjected.[4] Its importance also lies in the fact that pre-cooling reduces the energy requirement for subsequent refrigeration in cold rooms and the quality of refrigeration will be better since the food comes with a lower and homogeneous temperature (less temperature fluctuations).[1] Therefore, over time, a variety of food pre-cooling mechanisms have been used, including forced air, hydrocooling, cooling with liquid ice and vacuum cooling.[5]

One of the most used mechanisms is the one that uses forced air since it presents greater uniformity, by means of fans that allow the cold air pass through the food in an easier mode, increasing the rate of heat transfer by convection. In the pre-cooling process of fruits and vegetables, the forced air-cooling mechanism is usually used in cooling rooms since they allow the circulation of cold air and offer high capacity. However, the problem of non-homogeneity and energy consumption are always faced, which can be directly influenced by low air velocity and pressure loss. Other authors mention the influence of the opening ratio and, also the influence of parameters such as the distribution of the food inside the equipment (distance between products and stacking height).[6]

Likewise, factors such as size, proportion, and location of the ventilation holes on the upper, lower, and lateral faces of the packaging boxes[1,7] affect the physical-thermal and physiological properties of the product as well as the initial temperature.[8,9] However, the cooling process involves high energy consumption (59 kwh/MT). Fan operation and lighting are combined representing the 45 % of the electricity usage in an average cooler. Fruit cooling was only 36 % of the total electricity use. The electricity used to operate fans and remove the heat they produce is nearly equal to that used for fruit cooling.[4]

In cooling rooms, the cooling units are usually located on the roof, these are equipped with fans whose function is to blow cold air over the batteries. This job consumes 30 to 40 % of the total energy consumed. During the process, heat conduction occurs within the product, while heat and water exchanges take place at the air-product interface.[10]

Fans usually work at their highest power in the initial pre-cooling phase, once the food reaches the required temperature, the fans continue to run for an additional from 6 to 8 hours, which becomes an additional heat load. That is, air flow is one of the factors that determine the pre-cooling rate and the process efficiency, therefore energy consumption is a function of the power required to produce air flow through stacked packages and, the time required to maintain this airflow.[5] It is then necessary to know the behaviors of the air flow in order to develop techniques that allow to improve the uniformity of the air distribution in the refrigeration rooms, in the same way the optimization of the containers design or the stacking arrangement in cold rooms with the ultimate purpose of reducing energy consumption and product losses.[11]

Computational Fluid Dynamics (CFD) is a tool that allows aerodynamic and thermal analysis to be carried out in these cooling systems, thanks to it is possible to evaluate the factors previously mentioned that influence the efficiency of pre-cooling. Also, with the usage of equations such as Navier-Stokes with which mass, moment and energy balances are carried out,[8,12] with k-ε model being the most used. This model can help to improve these predictions by considering the anisotropy and the damping of turbulence near the wall, but they require much finer meshes.[10] Airflow patterns with resulting turbulence within a stacked product directly affect the heat transfer coefficient, thus the increase in the Nusselt number with increasing turbulence shows the importance of including the intensity of turbulence to model air flow and heat transfer.[13]

The experimental results obtained by [14] showed that the maximum air speed is found in the part near the top of the rear piles with a speed of the air exit of 4,8 ms-1, obtaining in this minor weight loss zone. Similarly, [11] demonstrated the differences that can be found in air velocity in a cooling room. They found that the speed was very low among the fruits, reaching values lower than 0,3 ms-1; while the air velocity in the upper part of the storage pile was significantly higher reaching values 7 times higher compared to what was recorded for the lower part of the piles. This problem has been previously reported by authors such as [10], who also reported that although the air speed was increased at the exit of the fan reaching very high values (5 to 10 ms-1), the air flow distribution is still heterogeneous.

To reduce the heterogeneity in the cooling rooms, authors such as [15] have used CFD to evaluate the effect of different loading patterns of cardboard containers filled with product. A study [16], they found that the design of vents in the packaging packages provide ventilation holes in the container that maintain an air flow channel between the environment and the interior of the container. They also mention that to maximize the uniformity of the cooling, the total opening areas must be large enough in order not to restrict the air flow. However, this is a parameter that must be studied carefully since authors such as [13] exposed that when the surface area of the openings covers 27 % of the container walls, the product becomes the largest contributor to pressure drop.

Therefore, the objective of this research was to evaluate the air flow influence of turbulence in the cooling rate of a fruit. First the model was validated against experimental data and then two factors were parameterized (bins open area and the mass air flow rate). A relationship between air flow, bin open area and local heat transfer coefficient will be established and linked with the cooling kinetics in terms of the 7/8th cooling time.

## METHOD
### Cold room Geometry
The cold room is shown in figure 1a. consists of a rectangular aluminum chamber with dimensions of 7,75 m (length) x 2,85 m (width) x 6,60 m (height). The cold room is the half of one used in the study of [11]. The cold rooms have two fans with a diameter inlet of 45 cm. The bins are organized in two rows, seven stacks and eight tiers. The dimensions of the bins is 120 cm (length) x 100 cm (width) x 78 cm (height). The initial bin open area was 900 cm2 in each side. For the parametric study, the lateral bin open area, figure 1a was parametrized from the initial value to 2500 cm2. This was made with the aim to study how this parameter affects effective thermal conductivity and 7/8th cooling time.

In stack 5 were placed two virtual fruits, figure 1b. One in the tier 1 and the other in tier 8. These virtual fruits were used to simulate the cooling rates. The physical properties of this virtual fruit as well the model is discussed in the following section.
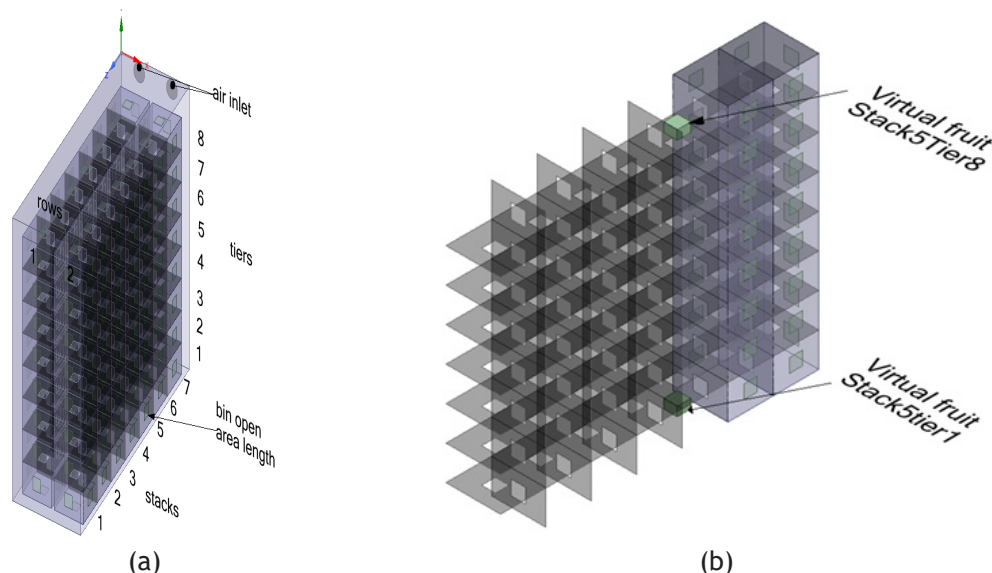


**Figure 1.** Cold room geometry (a) Virtual fruit locations (b)

### Mathematical model and numerical simulation
The airflow was modelled by the Reynolds Averaged Navier Stokes (RANS) equations with the continuity, momentum, and energy balance equations. The momentum and continuous equations were set for the air as follows:[17]

$$\frac{\partial \rho_a}{\partial t} + \nabla.(\rho_a \overrightarrow{v_a}) = 0 \tag{1}$$

$$\frac{\partial \rho_a \overrightarrow{v_a}}{\partial t} + \nabla.(\rho_a \overrightarrow{v_a} \overrightarrow{v_a}) = -\nabla.P_a + \nabla.(\bar{\bar{\tau}}) + \rho_a g \tag{2}$$

$$\bar{\bar{\tau}} = \rho_a \mu_t (\nabla.(\overrightarrow{v_a})) \tag{3}$$

$$\mu_t = \rho_a c_u \frac{\kappa^2}{\varepsilon} \tag{4}$$

Where, ρ is the density of air (Kgm-3); t is the time (s), $\overrightarrow{v}$ is the velocity (ms-1); $\bar{\bar{\tau}}$ is the tensor and $\mu t$ is the turbulent viscosity (Pa s); $cu$ is the turbulence model constant. The k-ε model was used to model the turbulence.[17] This model has been proven to be efficient in turbulence modeling.[18,19]

$$\frac{\partial \rho_a \kappa}{\partial t} + \nabla.(\rho_a \overrightarrow{v_a} \kappa_a) = \nabla.(\mu + \frac{\mu_t}{\sigma_\kappa}) \tag{5}$$

$$\frac{\partial \rho_a \varepsilon}{\partial t} + \nabla.(\rho_a \overrightarrow{v_a} \varepsilon) = \nabla.\left(\mu + \frac{\mu_t}{\sigma_\varepsilon}\right) + C_1 \frac{\varepsilon}{\kappa} G - C_2 \frac{\varepsilon^2}{\kappa} \tag{6}$$

Where, *keff* is the Effective thermal conductivity (W m-1 K-1); C1, C2, and C3 is the Turbulence model constant; G is the production of turbulence kinetic energy; T is temperature (°C). The modeled energy equation for the air is:

$$\rho_a C_{Pa} \frac{\partial T}{\partial t} + \partial T (\rho_a \overrightarrow{v_a} C_p T_a) = \nabla.(k_{eff} \nabla.T_a) \tag{7}$$

For k-ε model the effective thermal conductivity is given by:

$$k_{effa} = K_a + \frac{C_{pa} \mu_t}{P_{rt}} \tag{8}$$

Where in this case, is the thermal conductivity (*K*). The default value of the turbulent. Prandtl (Prt) number is 0,85. The model constants have the following default values: $cu$ = 0,09, C1 = 1,44, C2 = 1,92 and $\sigma k$ = 1$\sigma\varepsilon$ = 1,3. A porous media approach was used to calculate the flow pattern inside the bins. The momentum equation in the porous zone is:

$$\frac{\partial \alpha \rho_a \overrightarrow{v_a}}{\partial t} + \nabla.(\alpha \rho_a \overrightarrow{v_a} \overrightarrow{v_a}) = -\alpha \nabla.P + \nabla.(\alpha \bar{\bar{\tau}}) + \alpha \rho_a g - \left(\frac{\alpha^2 \mu}{\kappa_P} \overrightarrow{v_a} + \frac{\alpha^3 C_4}{2} \rho_a \frac{\alpha^2 \mu}{\kappa_P} \overrightarrow{v_a v_a}\right) \tag{9}$$

The last term in equation (9), represents the viscous and inertial forces imposed in the porous zones. The coefficients used in the pore zone were extracted of the work.[20] These values belong to a bin full of fruits table 1.

| Table 1. Pore zone coefficients and Fruit physical properties | | | | | | |
|---|---|---|---|---|---|---|
| **Property** | | | | | | |
| | $k_p$ (1/m²) | $C_4$ (1/m) | $\alpha$ | $\rho_s$ (kg/m³) | $C_p$ (J/kg K) | $K_{effs}$ (W/m K) |
| Value | 6,920,000 | 404 | 0,42 | 1,135 | 3,545 | 0,52 |

As it was explained before, two virtual fruits were place in stack 5. The cooling rates were just studied for these two virtual fruits because studying the kinetics in all the bins will be too expensive computationally as the simulation has to run in a transient mode. This will be explained deeply in results and discussion section. The modeled energy equation for the fruit is:

$$\rho_s C_{ps} \frac{\partial T_s}{\partial t} = \nabla.(\kappa \nabla.T_s) \tag{10}$$

The fruit physical properties were obtained from [1]. The date is summarized in table 1. This fruit was choice because they also present cooling kinetics that can be used to validate the kinetics curve trends. The initial temperature of the fruit was 17 °C, while the air temperature was 7 °C.

The boundary layer condition between the food and the air was modeled as follow:

$$\nabla.(\kappa\nabla.T_s) = \nabla.T_a\left(\left(K_a + \frac{C_{pa}\mu t_a}{P_{rta}}\right)\nabla.T_a\right) \qquad (11)$$

To capture all the phenomena in the boundary layer, the mesh in this zone were very fine. The equation (10) together with equation (11) and couple with the air fquation (1-9) were used to simulate the cooling kinetics.

The 7/8th time is three times the half-time for cooling. This value was calculated from the simulation results (cooling kinetics).

**Simulation strategy**

The boundary conditions were mass flow inlet. For the validation, the mass flow rate was set to 1,95 kgs-1. For the parametric study, the mass flow rate was studied in the range from this value to 0,65 kg / s with the objective of examining how this parameter affected effective thermal conductivity and 7/8th cooling time.

A non-slip boundary condition was used for all the walls. All models were solved with Fluent-ANSYS software using second-order upwind methods and a coupled pressure- velocity scheme. The COUPLE algorithm was used alongside a Fluent® solver to solve the pressure-velocity coupling equations.[17] The numerical model was run in transient mode with a time step of 180 and 300 interactions per time step.

*Model validation*

For the validation, the experimental data reported by [11] were taken to validate the local velocities in the cooling room as well as the velocities inside the bins. The mesh independency was made using the experimental local velocities. Three mesh were analyzed, and the local velocities presented the same results. Therefore, the coarse mesh shown in figure 2a with the inflation in the boundary layer figure 2b were used, in addition to the flow validation. The experimental data reported by [1] was used to validate the cooling kinetics trends.
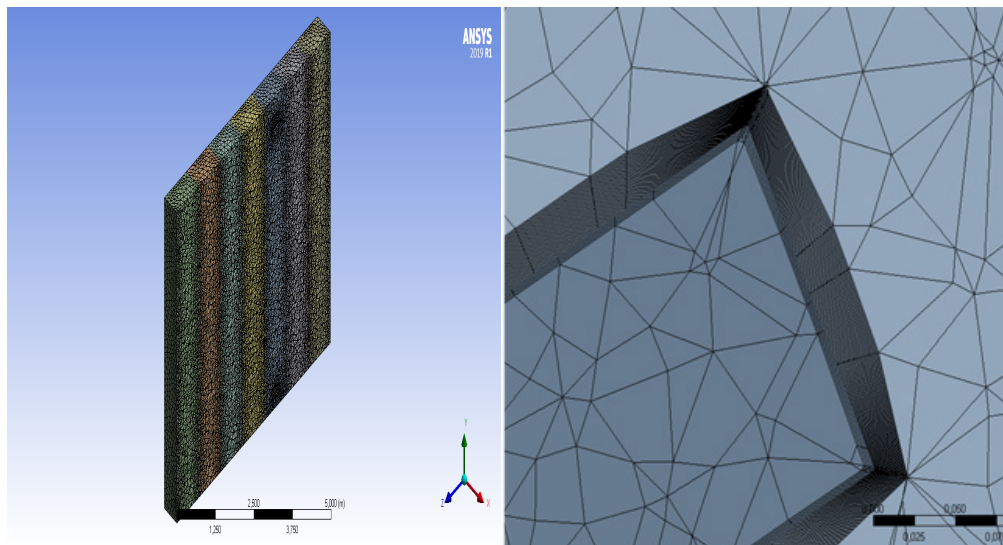


**Figure 2.** Cold room mesh (a) mesh inflation around the food (b)

**Parametric study and response variable**

The bins open area, and the mass flow rate were used in the parametric study. The sample points of these parameters were chosen by using central composite design. Central composite design (CCD) was based on 2-level factorial designs augmented with center and axial points to fit quadratic models. Regular CCDs have 5 levels for each factor.[21] Table 2 shows the sample points for which the response variable was calculated. Working with this type of experimental design, the sample points not only reduced the number of points required but also increased the accuracy of the response surface. For all sample points, the air inlet temperature was 7°C. With the values calculated with the CFD code, a surface was generated. Genetic aggregation was the default algorithm used to generate response surfaces.[17] The response variables in this work were ($keff$), it was the average of the effective thermal conductivity all nodes, which were calculated with equation (8) for each node.

| Sample point | Mass flow rate (kg/s) | Open area (cm²) | κ_effs (W/m K) | 7/8th cooling time Tier 8(h) | 7/8th cooling time Tier 1(h) | Difference Between Tier 8 and Tier 1 (h) |
|---|---|---|---|---|---|---|
| 1 | 1,315 | 1,500 | 7,66 | 8,85 | 15,45 | 6,60 |
| 2 | 1,315 | 900 | 7,44 | 9,00 | 15,30 | 6,30 |
| 3 | 1,315 | 2,100 | 7,72 | 9,15 | 14,45 | 5,30 |
| 4 | 0,680 | 1,500 | 5,91 | 11,11 | 17,10 | 6,00 |
| 5 | 1,950 | 1,500 | 9,19 | 7,95 | 14,40 | 6,40 |
| 6 | 0,680 | 900 | 5,72 | 10,35 | 17,10 | 6,70 |
| 7 | 0,680 | 2,100 | 6,27 | 11,40 | 16,95 | 5,50 |
| 8 | 1,950 | 900 | 8,97 | 8,10 | 14,70 | 6,60 |
| 9 | 1,950 | 2,100 | 9,58 | 8,70 | 13,35 | 4,60 |

**Table 2.** Design points (DOE)

## RESULTS AND DISCUSSION
### Model validation results

The figure 3 shows the results of the CFD simulation with respect to the experimental data obtained by [11]. The deviation of the predicted and experimental values was less than or equal to 14 %, which can be corroborated with what is observed in figure 4, where experimental and simulated air speeds in containers are shown at different levels for a mass flow rate of 1,95 kgs-1. Although there is an error between the experimental and simulated values, all the simulated ones are inside the experimental standard deviation.
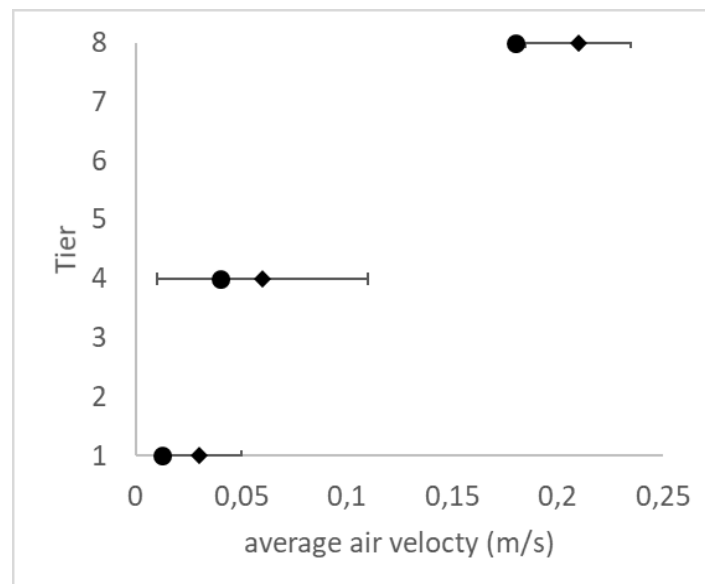


**Figure 3.** Experimental (diamonds)[11] and simulated (circles) air velocities in bins in different tiers. Air mass flow rate of 1,95 kg/s

The figure 4 shows that the 3D CFD that the data predicted with the model gave good results, according to the experimental data. According to the simulations carried out, the air speed was high when it met the first (upper) containers, and it decreased when it came into contact with the subsequent containers. In the simulation, in the same way, it was seen that the air course was in a descending circular way between row 1 and 2, this is shown in figure 4a. Similar results were obtained by [11] in their experiments and are shown in figure 4b. These showed that the course of air velocity decreased as it encountered the containers and with the fruit. Likewise, they observed a higher speed in the upper containers which decreased as it approached the nearby containers, however, they also evidenced an increase in the speed of the air that passed through the containers near the floor. Simulations carried out by authors such as [22] in CFD, showed a similar behavior in the air flow, showing that it had a swirling profile due to the rotation of the fan. When the air left the fan, it followed the upper part of the containers and afterwards hit the front wall and returned with high speed closed to the floor. The above was verified by [23], who modeled the cooling process within a cooling chamber with apples, they considered a cooling process with a vortex effect, obtaining a greater error in the theoretical versus experimental data when a model without a vortex effect was used (47 %), while with the vortex effect

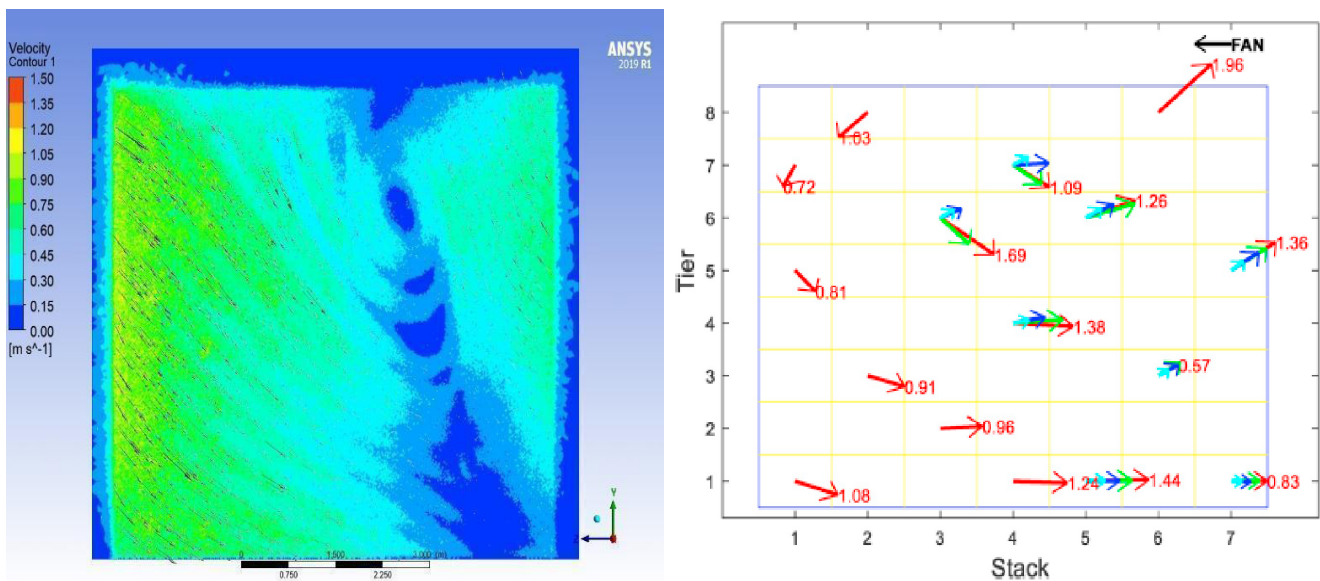they obtained an error of 27 %, greater than that obtained in this study.



**Figure 4.** Experimental flow and air velocities in the gap between two rows[11] (a) simulated velocities isocontours in the gap between two rows (b). Air mass flow rate of 1,95 kg/s

With the simulation carried out, hot areas corresponding to areas of less turbulence were detected as shown in figure 5, these areas, as reported by [22], usually presented a slow cooling due to poor air distribution, which in turn caused an acceleration of the biological deterioration processes and deteriorated general quality compared to areas of greater turbulence. This heterogeneity also resulted in a longer precooling period that resulted in higher operational cost.
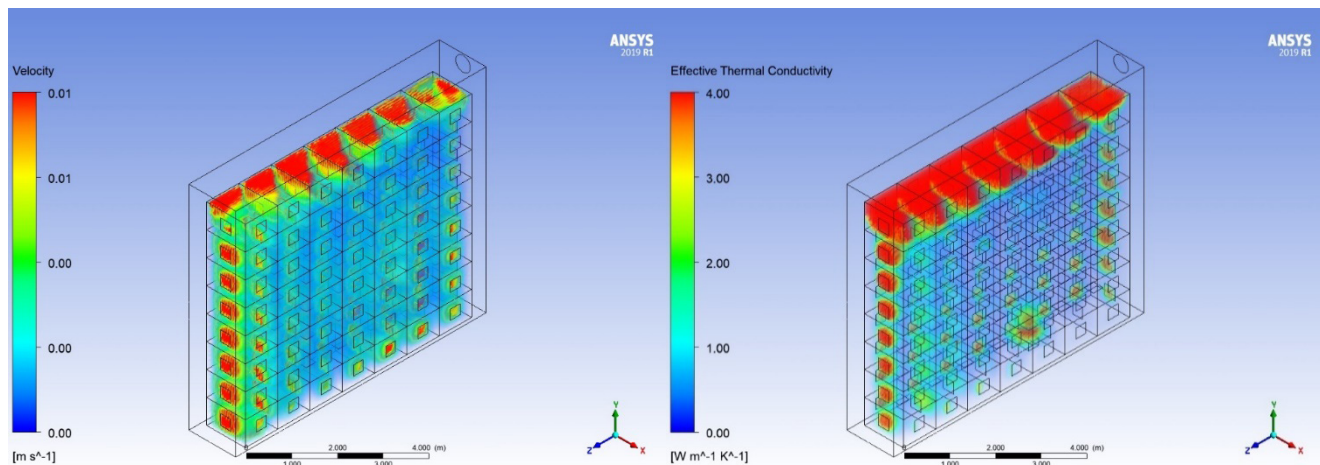


**Figure 5.** Isocontours of turbulence viscosity for air flow rate 1,95 kg/s. a) velocity and b) effective thermal conductivity

To test the model capability regarding the cooling kinetics, the experimental and simulated work done by [1] was taken to compare our simulation results. They analyzed a single layer of boxes arranged in three rows and with air flow range from 0,1 to 0,5ms-1 coming from the front (figure 6a). The diamonds showed the experimental kinetics in the pomegranate's boxes located in row 1 and the squares in the boxes located in row 3 (figure 6b). The continues and the dotted lines are the results in this work.

There are two points here to be analyzed, first, even if the cooling room in [1] is different from the cooling room in this work, the cooling curves have the same trends. Secondly, the authors, analyzed the heterogeneity horizontally (in the layer), in this work, the analysis is done in the vertical stratification (bin on the top and bin at the bottom) Also finding heterogeneity in the cooling curves. In both cases, the pressure loss reduced velocity, turbulence and therefore the local heat transfer coefficient.
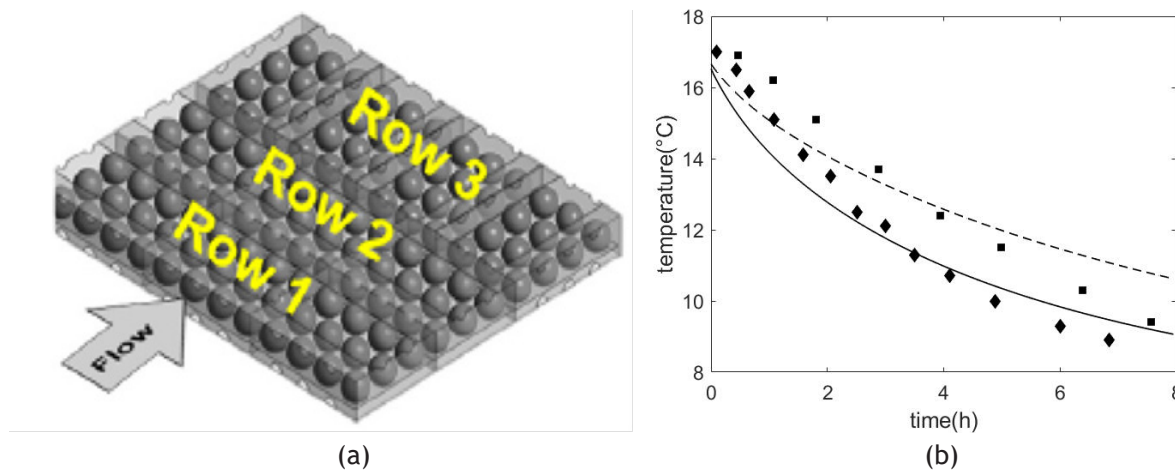
**Figure 6.** Boxes single layer configuration (a) Experimental (squares) (diamonds)[1] and simulated cooling kinetics in this work (Tier 8 stack - Continues line), (Tier 1 stack – dotted line). Air mass flow rate of 1,95 kg/s. Air temperature 7 °C. Initial Fruit temperature 17 °C (b)
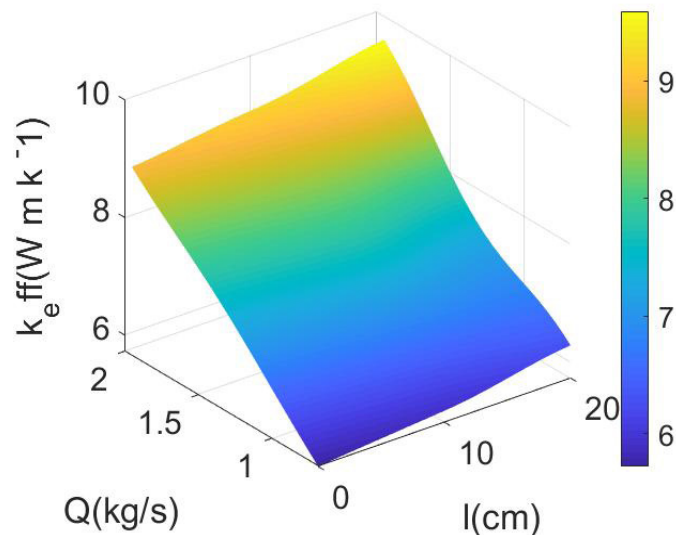
**Parametric study**



**Figure 7.** Surface response of Q and A vs effective thermal conductivity

The figure 7 shows that a decrease in mass flow rate had an increment in the 7/8th cooling time. This can be explained because there was a better heat transfer in the boundary layer between the air and the fruit. figure 8 shows also that the decrease in mass flow rate had a negative effect in the effective thermal conductivity. The right-hand term in equation (9) shows that effective thermal conductivity was the air thermal conductivity plus the turbulent thermal conductivity. So, increasing the air flow rate rose the turbulent thermal conductivity and therefore a better heat transfer in the boundary layer.[24] However, according to [24], an increase in the airflow rate implies the generation of a heat load of up to 50 % caused by the fan, which in turn increases the energy consumption of the refrigeration unit. It is important to highlight that to be able to capture the turbulence effects in the boundary layer, the mesh have to be very fine in this part of the geometry and therefore, for practical reasons, this can no be solved in the entire geometry. Solving the cooling kinetics in all parts of cooling room would demand a lot of computer resources and therefore in this work the virtual fruits were placed in the worst parts of cooling room. In terms of energy savings, decrease of the flow rate with a little increment in cooling could save energy but this must be coupled with the characteristics of the axial fan (rpm vs watts). [25] Regarding the open area of the silo, the increase in the open area showed an increase in the cooling time of 7/8 but with a reduction in the difference between the two silos, which could imply a better homogeneity as shown in figure 9.
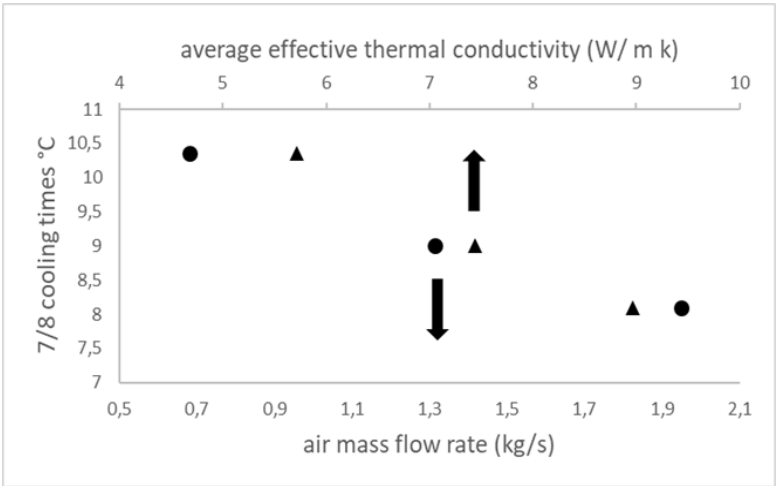
**Figure 8.** Relationship between mass flow rate and average effective thermal conductivity and 7/8 cooling times. Circles (air mass flow rate). Triangles (average effective thermal conductivity)
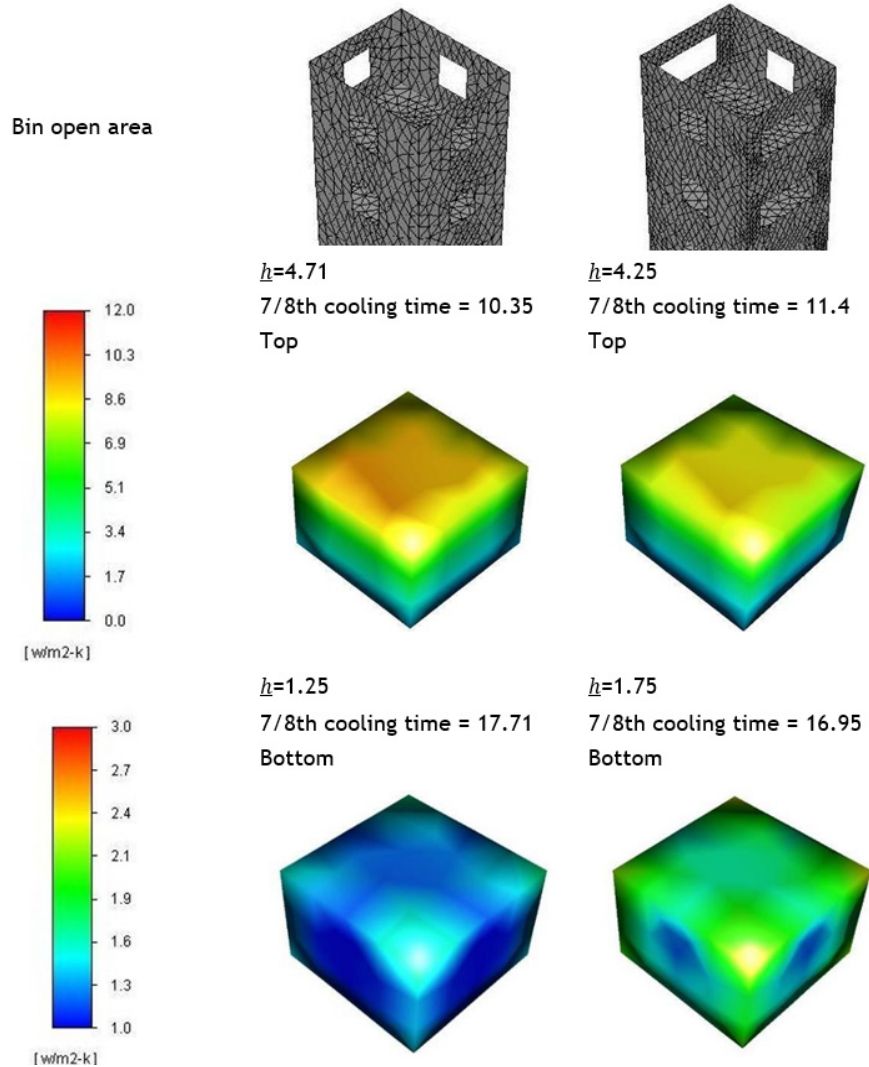


**Figure 9.** Comparison of local heat transfer at the surrounding of the virtual fruit

**Mapping the local heat transfer coefficient**

The increment in the cooling time with the reduction of flow rate was easy to correlate with the average effective thermal conductivity. However, for the bin open area better turbulence, better effective thermal conductivity and due to these conditions, a better local heat transfer coefficient was obtained.

Finally, as the cooling kinetics in all the space were difficult to characterize the local heat transfer could be a suitable response variable that helped to understand how changes in operation and geometry conditions impacted the cooling rate. Increments in the average heat transfer coefficient meant lower cooling rates however as it was space-average calculation it was not possible to predict with this variable the local to 7/8th cooling times. This value depended on the local values in the surroundings of the fruit as it is shown in figure 9. It is visible that the increments in bin area reduced the heterogeneity in the heat transfer coefficient and therefore the 7/8th cooling time. In other words, the gap between the cooling on the top at the bottom would be less pronounced, electricity usage for the forced- air cooling fans was controlled by the amount of air that must be moved to cool the fruit and the pressure drop the fans must operate against, and product cooling time. Increasing the bin open area could save energy due to reductions in pressure drop and therefore in heterogeneity which meant reductions in the general cooling time.[13]

## CONCLUSIONS

The use of 3D CFD allowed the obtention of adjusted data compared to experimental data reported by other authors with an error of 14 %. In this work, the distribution of the air flow reported by said authors was taken, where the air speed is higher in the upper areas of the first containers and lower as it approaches later containers. The simulation allowed to detect areas of less turbulence which in turn showed a low cooling rate and an increase in cooling time. Additionally, unlike works carried out by other authors who carry out the heterogeneity test in the horizontal direction, in this research it was carried out in the vertical direction, which showed that increasing the speed of the air flow increased the turbulent thermal conductivity, which improved heat transfer in the boundary layer. Additionally, conditions were obtained with which there is a small decrease in flow and an increase in cooling, which generates energy savings. Finally, increasing the open area by 57 % improves the homogeneity of cooling by reducing the difference in cooling time between the top and bottom.

## BIBLIOGRAPHIC REFERENCES

1.	Ambaw, A., Mukama, M., & Opara, U. L, 2017, "Analysis of the effects of package design on the rate and uniformity of cooling of stacked pomegranates: Numerical and experimental studies," Computers and Electronics in Agriculture, pp. 136, 13-24.

2.	Y. Duan, G.-B. Wang, O. A. Fawole, P. Verboven, X.-R. Zhang, D. Wu, U. L. Opara, B. Nicolai y K. & Chen, 2020, "Postharvest precooling of fruit and vegetables: A review," Trends in Food Science & Technology, n° 100, pp. 278-291.

3. Food and Agriculture Organization of the United Nations, 2011, "Global food losses and food waste," Düsseldorf.

4. Kitinoja, L., & Thompson, J. F., 2010, "Pre-cooling systems for small-scale producers," Stewart Postharvest Review An international journal for reviews in postharvest biology and technology.

5. Wang, G., & Zhang, X, 2020, "Evaluation and optimization of air-based precooling for higher postharvest quality: literature review and interdisciplinary perspective," Food Quality and Safety, vol. 4, n° 2, pp. 59-68.

6. L. R. de Castro, C. Vigneault, & L.A.B. Cortez., 2004, "Effect of Peripheral Openings on Cooling Efficiency of Horticultural Produce," American Society of Agricultural and Biological Engineers, 1 August.

7. Berry, T. M., Defraeye, T., Nicolaï, B. M., & Opara, U. L., 2016, "Multiparameter Analysis of Cooling Efficiency of Ventilated Fruit Cartons using CFD: Impact of Vent Hole Design and Internal Packaging," Food and Bioprocess Technology, vol. 9, n° 9, p. 1481–1493.

8. Delele, M. A., Ngcobo, M. E. K., Getahun, S. T., Chen, L., Mellmann, J., & Opara, U. L., 2013, "Studying airflow and heat transfer characteristics of a horticultural produce packaging system using a 3-D CFD model. Part I: Model development and validation," Postharvest Biology and Technology, pp. 536-545.

9. Tutar, M., Erdogdu, F., & Toka, B, 2009, "Computational modeling of airflow patterns and heat transfer prediction through stacked layers' products in a vented box during cooling," International Journal of Refrigeration, vol. 32, n° 2, pp. 295-306.

10. Mirade, P. S., Kondjoyan, A., & Daudin, J. D., 2002, "Three-dimensional CFD calculations for designing large food chillers," Computers and Electronics in Agriculture, vol. 34, n° 1-3, pp. 67-88.

11. Praeger, U., Jedermann, R., Sellwig, M., Neuwald, D. A., Hartgenbusch, N., Borysov, M., Truppel, I., Scaar, H., & Geyer, M., 2020, "Airflow distribution in an apple storage room," Journal of Food Engineering, vol. 269.

12. Liu, C. C., Ferng, Y. M., & Shih, C. K., 2012, "CFD evaluation of turbulence models for flow simulation of the fuel rod bundle with a spacer assembly," Applied Thermal Engineering, vol. 40, p. 389–396.

13. de Castro, L. R., Vigneault, C., & Cortez, L. A. B., 2005, "Cooling performance of horticultural produce in containers with peripheral openings," Postharvest Biology and Technology, vol. 38, n° 3, pp. 254-261.

14. Duret, S., Hoang, H.-M., Flick, D., & Laguerre, O., 2014, "Experimental characterization of airflow, heat and mass transfer in a cold room filled with food products," International, vol. 46, pp. 17-25.

15. Hung, D. van, Tong, S., Tanaka, F., Yasunaga, E., Hamanaka, D., Hiruma, N., & Uchino, T., 2011, "Controlling the weight loss of fresh produce during postharvest storage under a nano-size mist environment," Journal of Food Engineering, vol. 106, n° 4, pp. 325-330.

16. Pathare, P. B., Opara, U. L., Vigneault, C., Delele, M. A., & Al-Said, F. A. J., 2012, "Design of Packaging Vents for Cooling Fresh Horticultural Produce," Food and Bioprocess Technology, p. 2031–2045.

17. ANSYS, "ANSYS Fluent Tutorial Guide," January 2017. http://users.abo.fi/rzevenho/ansys%20fluent%20 18%20tutorial%20guide.pdf.

18. Dasore, A., & Konijeti, R., 2019, "Numerical Simulation of air Temperature and air flow Distribution in a Cabinet tray Dryer," International Journal of Innovative Technology and Exploring Engineering, vol. 8, p. 2278–3075.

19. Margaris, D. P., & Ghiaus, A. G., 2006, "Dried product quality improvement by air Flow manipulation in tray dryers," Journal of Food Engineering, vol. 75, n° 4, p. 542–550.

20. Scaar, H., Praeger, U., Gottschalk, K., Jedermann, R., & Geyer, M., 2017, "Experimental and numerical analysis of airflow in fruit and vegetable cold stores," LANDTECHNIK, vol. 72, n° 1, pp. 1-12.

21. Arjmandi, H., Amiri, P., & Saffari Pour, M., 2020, "Geometric optimization of a double pipe heat exchanger with combined vortex generator and twisted tape: A CFD and response surface methodology (RSM) study," Thermal Science and Engineering Progress, vol. 18.

22. Ghiloufi, Z., & Khir, T., 2019, "CFD modeling and optimization of pre-cooling conditions in a cold room located in the South of Tunisia and filled with dates," Journal of Food Science and Technology, vol. 56, pp. 3668-3676.

23. Hoang, H. M., Duret, S., Flick, D., & Laguerre, O., 2015, "Preliminary study of airflow and heat transfer in a cold room filled with apple pallets: Comparison between two modelling approaches and experimental results," Applied Thermal Engineering, vol. 76, pp. 367-381.

24. Wang, X. F., Fan, Z. Y., Li, B. G., & Liu, E. H., 2021, "Variable air supply velocity of forced-air precooling of iceberg lettuces: Optimal cooling strategies," Applied Thermal Engineering, vol. 187.

25. Prince, & Hati, A. S., 2021, "A comprehensive review of energy-efficiency of ventilation system using Artificial Intelligence," Renewable and Sustainable Energy Reviews, vol. 146.

## FINANCING

## CONFLICT OF INTEREST

Authors declare that there is no conflict of interest.

## AUTHORSHIP CONTRIBUTION

*Conceptualization:* Wilmer Cruz Guayacundo, Natali López Mejía, Hugo Fabian Lobatón García, Dustin Tahisin Gómez Rodríguez.

*Data curation:* Wilmer Cruz Guayacundo, Natali López Mejía, Hugo Fabian Lobatón García, Dustin Tahisin Gómez Rodríguez.

*Formal analysis:* Wilmer Cruz Guayacundo, Natali López Mejía, Hugo Fabian Lobatón García, Dustin Tahisin Gómez Rodríguez.

*Drafting - original draft:* Wilmer Cruz Guayacundo, Natali López Mejía, Hugo Fabian Lobatón García, Dustin Tahisin Gómez Rodríguez.

*Writing - proofreading and editing:* Wilmer Cruz Guayacundo, Natali López Mejía, Hugo Fabian Lobatón García, Dustin Tahisin Gómez Rodríguez.

<p align="center" style="color:red"><b>ANNEXES</b></p>

**Nomenclature**

| | |
|---|---|
| $\underline{k}_{eff}$ | effective thermal conductivity, W/ m k |
| $k_{eff}$ | average effective thermal conductivity, W/ m k |
| T | temperature, k |
| t | time, s |
| $\mu_t$ | turbulence viscosity, Pa s |
| G | production of turbulence kinetic energy |
| Ai | volume where the variable is evaluated, $m^3$ |
| $C_1$ | turbulence model constant |
| $C_2$ | turbulence model constant |
| $C_u$ | turbulence model constant |
| | velocity, m/s |
| g | gravitational acceleration, $m/s^2$ |
| K | thermal conductivity, W/m k |
| P | pressure, atm |
| $C_4$ | inertial resistance, 1/m |
| | Sheer stress tensor $N/m^2$ |
| $C_p$ | specific heat capacity J/Kg°c |
| | model constants in standard k-epsilon model |
| | model constants in standard k-epsilon model |
| $P_{rt}$ | Prandtl number |
| | Permeability parameter |
| | Velocity vector (m/s) |
| **Greek Letters** | |
| | uniformity index |
| | Density, $kg/m^3$ |
| | k-epsilon (k-ε) model |
| | k-epsilon (k-ε) model |
| | Viscosity N s / $m^2$ |
| | Void fraction |
| **Sub index** | |
| a | air |
| s | food, solid |
| **Acronyms and abbreviations** | |
| CFD | computational fluid dynamics |
| DOE | design of experiments |
| RSM | response surface methodology |